PROCEEDINGS OF THE INTERNATIONAL CONFERENCE NANOMATERIALS: APPLICATIONS AND PROPERTIES
Vol. **2** No 4, 04NEA06(4pp) (2013)

High-rate Electrochemical Performance of Nanosized $LiNi_{0,5}Mn_{1,5}O_4$

A.V. Potapenko[1], S.I. Chernukhin[1], I.V. Romanova[2], K.Sh. Rabadanov[3], M.M. Gafurov[3], S.A. Kirillov[1,2,*]

[1] *Joint Department of Electrochemical Energy Systems, 38A, Vernadsky Ave., 03142 Kyiv, Ukraine*
[2] *Institute for Sorption and Problems of Endoecology, 13, Gen. Naumov Str., 03164 Kyiv, Ukraine*
[3] *Kh.I. Amirkhanov Institute of Physics and Analytical Center of Common Access, 94, M. Yaragsky Str., 367003 Makhachkala, Russian Federation*

(Received 20 May 2013; published online 31 August 2013)

Structural and electrochemical characteristics of nanosized $LiNi_{0,5}Mn_{1,5}O_4$ synthesized by means of a citric acid aided route are presented. It is found that materials treated at 800 °C consist of the maximal amount of the disordered face-centered cubic phase. Galvanostatic discharge curves registered at various discharge currents (147-5800 mA·g^{-1} or 1-40 C) prove the excellent high-rate performance of the samples studied. Specifically, the sample treated at 800 °C endures a load of 40 C delivering the reversible specific capacity of 34 mAh·g^{-1}. Such results have never been attained with $LiNi_{0,5}Mn_{1,5}O_4$ electrodes prepared using standard techniques and overwhelms all existing data published to date. This remarkable result makes evident excellent prospects of non-solid-state routes for obtaining electrode materials for heavy-duty lithium-ion batteries of new generation.

Keywords: $LiNi_{0,5}Mn_{1,5}O_4$, Lithium-ion batteries; High-rate performance.

PACS numbers: 82.47.Aa, 82.45.Yz

1. INTRODUCTION

The lithium-manganese spinel $LiMn_2O_4$ has been introduced in electrochemical practice in 1983 [1] and since that time attracts much attention of experimentalists. One of approaches enabling one to expand electrochemical parameters of lithium-manganese spinels is doping its structure with transition metal ions thus getting various compounds of the general formula of $LiMe_{1-x}Me_xO_4$ [2]. Another, more general approach equally applicable either to cathode and anode materials of lithium-ion power sources is obtaining them in a nanosized form [3]. Subdivision leads to great increasing the area of contact between electrode and electrolyte and decreasing distances passed by electrons and lithium ions upon diffusion in the electrode material. This allows for improving cycleability and attaining greater discharge rates than in the case of the electrode materials of a large particle size.

Amidst well known materials of $LiMe_{1-x}Me_xO_4$ composition those doped with Me = Ni, Cr, Co, Fe, Cu are of the greatest interest [4-7]. The Ni-doped derivative of $LiNi_{0,5}Mn_{1,5}O_4$ composition seems the most prospective among them. The thing is that unlike other dopants, the oxidation potential of nickel ($Ni^{2+} \rightarrow Ni^{4+}$) is lower than 4.8 V, thus decreasing the probability of electrolyte decomposition on the surface of an electrode material. The theoretical specific capacity of $LiNi_{0,5}Mn_{1,5}O_4$ equals to 146.7 mAh·g^{-1}. Practical specific capacities for $LiNi_{0,5}Mn_{1,5}O_4$ lie within 130-140 mAh/g [8, 9], as opposed to other doped lithium-manganese spinels, for which those are much smaller.

Non-substituted lithium-manganese spinels are known to belong to the *Fd*3*m* space group, $Z = 8$ [10, 11]. $LiNi_{0,5}Mn_{1,5}O_4$ can belong to one of two space groups, viz., the ordered primitive cubic $P4_332$ and the disordered face-centered cubic *Fd*3*m* [12, 13]. In the ordered phase, the Mn^{4+} and Ni^{2+} ions fill octahedral positions with the ratio of 3 : 1. In the disordered one, both cations are distributed randomly. As the scattering coefficients of nickel and manganese are very close, distinguishing between these crystalline phases by means of X-ray diffraction data is problematic, and the methods of vibrational spectroscopy are helpful in solving this problem [14, 15]. On the other hand, the nanosized disordered $LiNi_{0,5}Mn_{1,5}O_4$ demonstrates higher electronic conductivity than the ordered one [16].

Important factors influencing the electrochemical parameters of the doped spinels and associated with their crystal structure are the temperature and time of a heat treatment [13-15, 17]. The $LiNi_{0,5}Mn_{1,5}O_4$ samples annealed at $t < 700$ °C are ordered, and annealing at $t > 700$ °C gives the disordered structure [15].

Optimal samples of $LiNi_{0,5}Mn_{1,5}O_4$ obtained by means of solid-state procedures reveal good rate capabilities. For example, being loaded with the specific currents of 1470 mA·g^{-1} (10C) model Li | $LiNi_{0,5}Mn_{1,5}O_4$ cells demonstrate the specific capacities of ~ 113 mAh·g^{-1} [18] and 104 mAh·g^{-1} [19], and the higher the loads, the smaller the capacities: 2205 mA·g^{-1} (15 C) and 80 mAh·g^{-1} [20] and 2930 mA·g^{-1} (20 C) and 40 mAh·g^{-1} [21].

In our previous papers [22, 23], a modified citric acid route has been elaborated for obtaining nanosized materials for catalysis [24] and electrochemistry [25]. It is tempting to apply a similar route to $LiNi_{0,5}Mn_{1,5}O_4$.

It should be mentioned that attempts to obtain $LiNi_{0,5}Mn_{1,5}O_4$ for lithium-ion batteries by means of the citric acid route are already known [26, 27] but heavy-duty properties of materials obtained are limited by discharge currents values of about 735 mA·g^{-1} (5 C) [26, 27].

In this paper, we report on the citric acid aided syn-

* kir@i.kiev.ua

thesis and characterization of $LiNi_{0,5}Mn_{1,5}O_4$, and electrochemical studies of cathodes made of it, with special reference to the ability of discharging the cathodes with great currents.

2. EXPERIMENTAL

Citrate precursors were synthesized by means of a procedure described in Refs. [22-24]. To select proper temperatures of pyrolysis and annealing of pyrolyzed samples, thermal analysis studies (Q-1500 D, MOM, Hungary) were applied. Specific surface areas were measured on an ASAP device (Micromeritics, USA). IR spectra were registered on a VERTEX 70 Fourier spectrometer (Bruker, USA) operating in a reflection mode; at least 64 scans were accumulated. Phase composition, morphology and particle sizes were analyzed by X-ray diffraction (DRON-4-07, LOMO, Russia, Co K_α radiation) and electron scanning microscopy (JSM-6700F, JEOL, Japan).

Electrochemical measurements were performed as described in Ref. [28], on a home-made automated electrochemical workstation using cyclic voltammetry and galvanostatic charge / discharge cycling methods. Sample 2016 coin cells with a lithium metal anode serving as a counter and reference electrode, a cathode made of the material in question, a Celgard 2500 separator membrane and a 1 mol / L solution of $LiPF_6$ in a mixture of ethylene carbonate / diethyl carbonate with the mass ratio of 1 : 1 were assembled. The working electrode was made of 82 % of the material under consideration, 10 % of a conducting additive (carbon black) and 8 % of a binder (poly(vinylidene difluoride)). Parameters of discharge were expressed in C [mA/g] values.

3. RESULTS AND DISCUSSION

Thermal decomposition data for the citrate precursor of $LiNi_{0,5}Mn_{1,5}O_4$ are shown in Fig. 1. The main mass loss region (ca. 80 %) occurs at temperatures lower than 400 °C being due to the removal of water at 100-150 °C, and the strongly exothermic breakup of organic radicals and decomposition of their fragments (burning) taking place at $t > 320$ °C.

Based on this data, precursors were treated in the following way. The temperature of pyrolysis was chosen as 400 °C. The annealing temperatures were selected as 600, 700, 750, and 800 °C.

X-ray diffraction data for $LiNi_{0,5}Mn_{1,5}O_4$ samples thermally treated at various temperatures are presented in Fig. 2. Reflections from the (111), (311), (400) and (440) planes are peculiar for the $LiMn_{1,5}Ni_{0,5}O_4$ structure (JCPDS 32-0581). Small maxima appearing between the (222) and (400) peaks are due to the presence of an admixture of NiO (JCPDS 4-835).

The values of crystallite size $d_{cryst.}$ calculated in terms of Scherrer [29] and Holland-Redfern methods [30] are collected in Table 1. Clearly, a growth of crystallites and healing of structure inhomogeneities showing up in the compaction of the sample occur upon heating.

The values of specific surface area (3.8-7.2 m^2/g) and pore volume (0.02-0.04 cm^3/g) of the samples well agree with existing data [31] and reveal low porosity and the high degree of crystallite aggregation of materials.

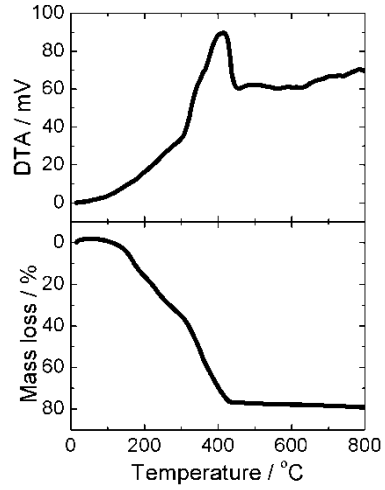

Fig. 1 – Thermal analysis of citrate precursor of $LiNi_{0,5}Mn_{1,5}O_4$ spinel

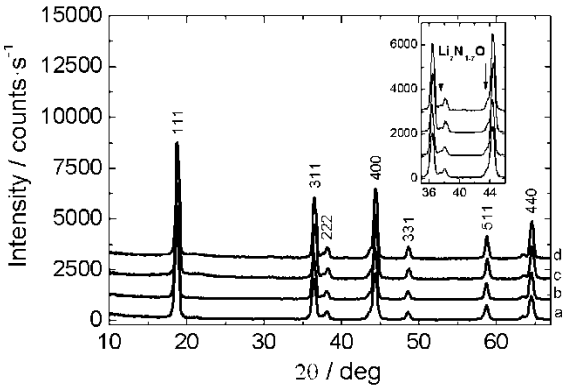

Fig. 2 – X-ray diffraction data for $LiNi_{0,5}Mn_{1,5}O_4$ treated at various temperatures. a – 600 °C; b – 700 °C; c – 750 °C; d – 800 °C

Table 1 – Parameters of nickel doped lithium-manganese spinel treated at various temperatures

Annealing temperature, °C	$d_{cryst.}$, nm	a, nm	V, Å^3
600	15	0.8180	0.5474
700	16	0.8182	0.5477
750	22	0.8175	0.5464
800	20	0.8169	0.5452

SEM micrographs of the fired samples are given in Fig. 3. Their examination reveals that the samples annealed at 750 °C consist of loosely packed, imperfect crystals. At 800 °C, the crystallization process is finishing, and closely packed, perfectly shaped crystals of < 200 nm size and the octahedral and cubo-octahedral habit are forming.

In order to understand if nickel-manganese spinels thermally treated at various temperatures are ordered ($P4_332$) or disordered ($Fd3m$), IR spectra in the region of 400-700 cm^{-1}, where the vibrations of metal-oxygen bonds in the crystal are showing up, should be analyzed [14-16]. As shown in Ref. [16], the ratio of intensities of IR bands at ~ 619 and ~ 588 cm^{-1} is a criterion of structure ordering. In our case, these bands appear at 621 and 583 cm^{-1} (Fig. 4). According to their inten-

sities, the samples annealed at 400 and 600 °C are ordered, and those treated at 750 and 800 °C are disordered.

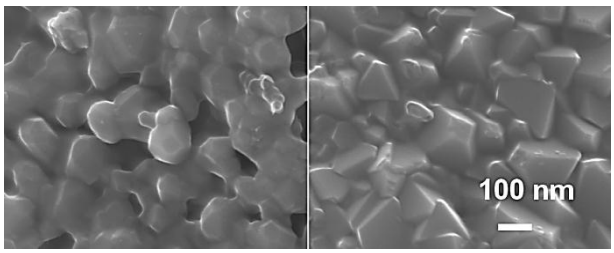

Fig. 3 – SEM micrographs of $LiNi_{0,5}Mn_{1,5}O_4$ samples upon thermal treatment at 750 °C (left) and 800 °C (right)

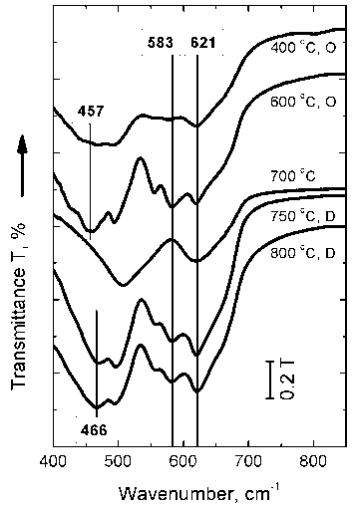

Fig. 4 – IR spectra of $LiNi_{0,5}Mn_{1,5}O_4$ samples thermally treated at various temperatures

In Fig. 5, stationary cyclic voltammetry curves for $LiNi_{0,5}Mn_{1,5}O_4$ electrodes are presented. In both cathode and anode regions, all electrodes demonstrate two intense main peaks at 4.6-4.7 V and a weak diffuse peak at around 3.85-4.3 V. The main anodic peaks correspond to the consecutive oxidation of Ni^{2+} to Ni^{3+} and Ni^{3+} to Ni^{4+}, and the cathodic peaks reflect respective backward reactions. As follows from their shapes, upon the thermal treatment at higher temperatures, the better resolution of the main peaks and the higher current values are achieved signifying better electrochemical properties of the samples. Diffuse peaks at lower potential values may correspond to the working region of the mother $LiMn_2O_4$ spinel [17].

Galvanostatic discharge curves at various discharge currents (1-40 C) are demonstrated in Fig. 6. Charge rates are 1 C with an additional charge at 0.1 C applied. Dependences of the specific capacities of $Li|LiNi_{0,5}Mn_{1,5}O_4$ cells with cathodes prepared using spinels of different thermal pre-history on the discharge current are clearly different. The specific capacities at zero current for cells with electrodes treated at different temperatures significantly vary being equal to 75 mAh·g^{-1} at 600 °C, 95 mAh·g^{-1} at 700 °C, and ~ 105 mAh·g^{-1} at 750 and 800 °C. The specific capacities attainable upon high loads for electrodes prepared from materials annealed at lower temperatures (600 and 700 °C) are smaller than those for electrodes prepared from materials annealed at higher temperatures (750 and 800 °C). The sample thermally treated at 800 °C is able to endure a load of 5800 mAh·g^{-1} (40 C) delivering the reversible specific capacity of 34 mAh·g^{-1}. At the current density of ~ 4000 mAh·g^{-1} (27 C), its reversible specific capacity equals to the half of the theoretical specific capacity of the material (73 mAh·g^{-1}). This outmatches all existing data regarding Ni-doped lithium-manganese spinels [26, 27, 32, 33].

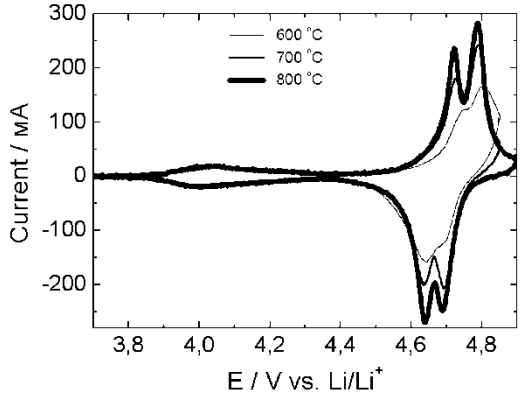

Fig. 5 – Stationary cyclic voltammetry curves for $LiNi_{0,5}Mn_{1,5}O_4$ electrodes prepared from samples thermally treated at 600, 700, 750, and 800 °C. Scanning rate 0.1 mV/s

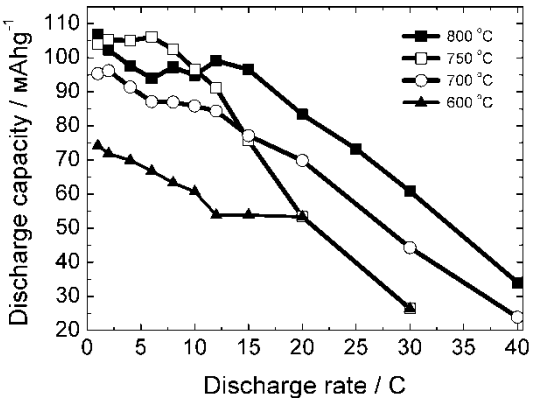

Fig. 6 – Dependence of the specific capacity of $LiNi_{0,5}Mn_{1,5}O_4$ samples annealed at various temperatures on the specific density of discharge current expressed in C units (1 C = 146.7 mAh·g^{-1})

4. CONCLUSION

In this paper, we described the citric acid aided synthesis of the nanosized nickel-doped lithium manganese spinel, $LiNi_{0,5}Mn_{1,5}O_4$, and its physico-chemical and electrochemical characterization. X-ray diffraction, scanning electron microscopy and IR spectroscopy enabled us to discern between ordered and disordered phases of the target product, and to conclude that being annealed at the temperatures of 600-800 °C, the optimal electrode materials could be obtained upon the thermal treatment at 800 °C. Specifically, in spite of the similar values of unit cell parameters 0.8175 nm, specific surfaces 6.88 m^2/g, particle sizes 16 nm for all thermally treated materials, those annealed at 800 °C

consisted of the maximal amount of the disordered face-centered cubic phase. The stationary cyclic voltammetry curves demonstrated the better resolution of the main cathodic and anodic peaks for cathodes made of disordered materials treated at 800 °C signifying their better electrochemical properties. Galvanostatic discharge curves registered at various discharge currents (147-5800 $mAh \cdot g^{-1}$ or 1-40 C) proved excellent high-rate performance of the materials obtained. The sample thermally treated at 800 °C was able to endure a load of 5800 $mAh \cdot g^{-1}$ (40 C) delivering the reversible specific capacity of 34 $mAh \cdot g^{-1}$. At the current density of ~ 4000 $mAh \cdot g^{-1}$ (27 C), its reversible specific capacity was equal to the half of the theoretical specific capacity of the material (73 $mAh \cdot g^{-1}$), and at the loads of 20, 15 and 10 C, both this and even other materials thermally treated in non-optimal way overwhelmed all existing data published to date in the scientific literature. This remarkable result made evident excellent prospects of non-solid-state routes for obtaining electrode materials for heavy-duty lithium-ion batteries of new generation.

ACKNOWLEDGMENT

IR data have been obtained in Analytical Center of Common Access supported by the Russian Federation Basic Research Fund (Grant #13-03-00384A) and the Ministry of Education and Science of the Russian Federation (State Contract #16.552.11.7092).

REFERENCES

1. M.M. Thackeray, W.I.F. David, P.G. Bruce, *Mater. Res. Bull.* **18**, 461 (1983).
2. Y. Ein-Eli, W.F. Howard, S.H. Lu, S. Mukerjee, J. McBreen, J.T. Vaughey, M.M. Thackeray, *J.Electrochem. Soc.* **145**, 1238 (1998).
3. A.S. Aricò, P. Bruce, B. Scrosati, J.-M. Tarascon, Walter van Schalkwijk, *Nat. Mater.* **4**, 366 (2005).
4. H.M. Wu, J.P. Tu, Y.F. Yuan, J.Y. Xiang, X.T. Chen, X.B. Zhao, G.S. Cao, *J. Electroanal. Chem.* **608**, 8 (2007).
5. J.M. Amarilla, R.M. Rojas, F. Pico, L. Pascual, K. Petrov, D. Kovacheva, M.G. Lazarraga, I. Lejona, J.M. Rojo, *J. Power Sources* **174**, 1212 (2007).
6. Y. Ein-Eli, J.T. Vaughey, M.M. Thackeray, S. Mukerjee, X.Q. Yang, J. McBreen, *J. Electrochem. Soc.* **146**, 908 (1999).
7. T.-F. Yi, C.-Y. Li, Y.-R. Zhu, R.-S. Zhu, J. Shu, *Russ. J. Electrochem.* **46** No2, 227 (2010).
8. H.-S. Fang, Z.-X. Wang, X.-H. Li, H.-J. Guo, W.-J. Peng, *J. Power Sources* **153**, 174 (2006).
9. T. Ohzuku, S. Takeda., M. Iwanaga, *J. Power Sources* **81-82**, 90 (1999).
10. M.H. Rossouw, A. de Kock, L.A. de Piciotto, W.I.F. David, R.M. Ibberson, *Mater. Res. Bull.* **25**, 173 (1990).
11. M.M. Thackeray, P.J. Johnson, L.A. de Picciotto, P.G. Bruce, J.B. Goodenough, *Mater. Res. Bull.* **19**, 179 (1984).
12. N. Amdouni, K. Zaghib, F. Gendron, A. Mauger, C.M. Julien, *Ionics* **12**, 117 (2006).
13. J.-H. Kim, S.-T. Myung, C.S. Yoon, S.G. Kang, Y.K. Sun, *Chem. Mater.* **16**, 906 (2004).
14. R. Alcantara, M. Jaraba, P. Lavela, J.L. Tirado, E. Zhecheva, R. Stoyanova, *Chem. Mater.* **16**, 1573 (2004).
15. M. Kunduraci, J.F. Al-Sharab, G.G. Amatucci, *Chem. Mater.* **18**, 3585 (2006).
16. M. Kunduraci, G.G. Amatucci, *J. Electrochem. Soc.* **153**, A1345 (2006).
17. D. Pasero, N. Reeves, V. Pralong, A.R. West, *J. Electrochem. Soc.* **155**, A282 (2008).
18. X.Y. Feng, C. Shen, X. Fang, C.H. Chen, *J. Alloy. Compd.* **509**, 3623 (2011).
19. X.-Y. Feng, C. Shen, X. Fang, C.-H. Chen, *Chinese Sci. Bull.* **57**, 4176 (2012).
20. J.C. Arrebola, A. Caballero, L. Hernán, J. Morales, *J. Nanomater.* **16**, No1, 1 (2008).
21. H.-W. Lee, P. Muralidharan, M.M. Claudio, R. Ruffo, D.-K. Kim, *J. Power Sources* **196**, 10712 (2011).
22. I.A. Farbun, I.V. Romanova, T.E. Terikovskaya, D.I. Dzanashvili, S.A. Kirillov, *Russ. J. Appl. Chem.* **80** No11, 1798 (2007).
23. I.A. Farbun, I.V. Romanova, S.A. Kirillov, *J. Sol-Gel Sci. Technol.* DOI 10.1007/s10971-013-3024-7 (2013).
24. I.V. Romanova, I.A. Farbun, S.A. Khainakov, S.A. Kirillov, V.A. Zazhigalov, *Rep. Natl Acad. Sci. Ukraine* **154** No10, (2008).
25. A.V. Potapenko, S.I. Chernukhin, I.V. Romanova, S.A. Kirillov, *Chemistry, Physics and Technology of Surface* **2** No2, 175 (2011). [in Russian].
26. T. Yang, N. Zhang, Y. Lang, K. Sun, *Electrochim. Acta* **56**, 4058 (2011).
27. N. Zhang, T. Yang, Y. Lang, K. Sun, *J. Alloy. Compd.* **509**, 3783 (2011).
28. S.A. Kirillov, T.V. Lisnycha, S.I. Chernukhin, *J. Power Sources* **196**, 2221 (2011).
29. A. Patterson, *Phys. Rev.* **56**, 978 (1939)
30. T.J.B. Holland, S.A.T. Redfern, *Mineralogical Magazine* **61** No1, 65 (1997).
31. M.-S. Kuthanapillil, P.-G. Bruce, *Dalton Trans.* **40** No1, 5471 **(**2008).
32. O. Sha, Z. Tang, S. Wang, W. Yuan, Z. Qiao, Q. Xu, L. Ma, *Electrochim. Acta* **77**, 250 (2012).
33. C.Q. Feng, H. Li, C.F. Zhang, Z.P. Guo, H.M. Wu, J. Tang, *Electrochim. Acta* **61**, 87 (2012).